Method of model reduction and multifidelity models for solute transport in random layered porous media

Zhijie Xu* and Alexandre M. Tartakovsky
Computational Mathematics Group, Physical & Computational Sciences Directorate, Pacific Northwest National Laboratory, Richland, Washington 99354, USA
(Received 16 June 2017; published 28 September 2017)

This work presents a method of model reduction that leads to models with three solutions of increasing fidelity (multifidelity models) for solute transport in a bounded layered porous media with random permeability. The model generalizes the Taylor-Aris dispersion theory to stochastic transport in random layered porous media with a known velocity covariance function. In the reduced model, we represent (random) concentration in terms of its cross-sectional average and a variation function. We derive a one-dimensional stochastic advection-dispersion-type equation for the average concentration and a stochastic Poisson equation for the variation function, as well as expressions for the effective velocity and dispersion coefficient. In contrast to the linear scaling with the correlation length and the mean velocity from macrodispersion theory, our model predicts a nonlinear and a quadratic dependence of the effective dispersion on the correlation length and the mean velocity, respectively. We observe that velocity fluctuations enhance dispersion in a nonmonotonic fashion (a stochastic spike phenomenon): The dispersion initially increases with correlation length λ, reaches a maximum, and decreases to zero at infinity (correlation). Maximum enhancement in dispersion can be obtained at a correlation length about 0.25 the size of the porous media perpendicular to flow. This information can be useful for engineering such random layered porous media. Numerical simulations are implemented to compare solutions with varying fidelity.

DOI: 10.1103/PhysRevE.96.033314

I. INTRODUCTION

Many scientific applications (e.g., barotropic flow, contaminant transport, and functionally graded materials) are multiscale and stochastic in nature with uncertainties stemming from random initial and/or boundary conditions and/or stochastic parameter fields. Solving these stochastic problems is both theoretically and computationally challenging.

Most existing approaches to solute transport in heterogeneous media compute the lower-order moments of concentration. Perturbation-based moment methods for solving stochastic advection-dispersion equations develop nonphysical bimodal behavior for average concentration [1,2]. The moment solution based on the macrodispersion theory [3] requires knowledge of Green's function, which is expensive to compute numerically and can only be found analytically for a small class of problems (e.g., infinite domains). Another drawback to these methods is that their accuracy rapidly deteriorates with increasing variance of the random parameters (i.e., advection velocity and/or dispersion coefficient). Other methods focus on deriving the evolution equations for probability density functions of concentration that contain more complete information than moment-based methods [4]. An assumption of negligible transverse dispersion has to be made in order to obtain explicit expressions for layered heterogeneous media. Other statistical approaches, including Monte Carlo methods, suffer from a low convergence rate [$O(N^{-1/2})$, where N is the number of samples] and are destined to fail when directly applied to problems with large numbers of degrees of freedom [5].

Polynomial-chaos-based methods [6–8] currently are the best choice for quantifying uncertainty [9–11]. However, these methods suffer from the so-called curse of dimensionality and become prohibitively expensive when applied to problems with correlated-in-space random parameters characterized by small correlation length and/or large variance [12–18].

In this paper we present a reduction method for solute transport in layered heterogeneous porous media with a random distribution of the hydraulic conductivity across the layers. We derive stochastic equations for the spatial average of concentration and variations around the average. The spatial average represents the large-scale concentration and is governed by a stochastic advection-dispersion equation with the effective stochastic advection velocity and dispersion coefficient. The small-scale variability of the concentration, caused by the small-scale velocity fluctuations, is captured by the variation function, depending on the velocity covariance. The resulting hierarchical stochastic models enable efficient solutions of the original problem with significantly reduced dimensionality.

Taylor and Aris's classical dispersion theory was developed for long-time evolution of solute concentration [19–21] (see also [22–29]). Whitaker, Adler, Brenner, and later Bear generalized this theory to (deterministic) flow in porous media. Neuman [3] and Koch and Brady [30] derived deterministic effective dispersion equations for solute transport in the stochastic velocity field. Our method generalizes the Taylor dispersion theory [19,20] for transport in the stochastic velocity field. Unlike Neuman's macrodispersion theory [3] (which results in deterministic macroscale equations), our method yields a stochastic macroscale advection-dispersion equation and an expression for microscale concentration fluctuations. A stochastic form of the effective equation allows efficient uncertainty quantification and parameter and state estimations using small-scale concentration measurements.

In the proposed method, for known statistics of the advective velocity, the variation function, effective advection

*zhijie.xu@pnnl.gov

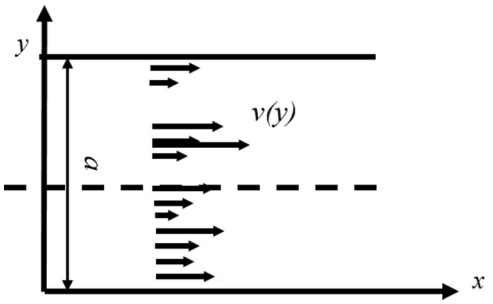

FIG. 1. Flow confined by two parallel plates with a stochastic velocity profile $v(y)$.

velocity, and effective dispersion coefficient can be computed analytically. The stochastic parameters in the effective equation have smaller variance and larger correlation lengths than their small-scale counterparts in the original advection-dispersion equations. Therefore, the effective stochastic equation can be solved using Monte Carlo simulations (MCSs) with significantly coarser resolution than the one required in the MCS solution for the original equation. In addition, as the accuracy of these methods increases with decreasing variance of the random parameters in the stochastic equations, the moment equation and macrodispersion methods should be more accurate for the effective equation than for the original equations.

II. FORMULATION OF THE MODEL

Here we consider solute transport in porous media consisting of homogeneous layers with random permeability distribution across the layers. The randomness in permeability leads to randomness of the advective velocity. The two-dimensional (2D) geometry of the problem is defined in Fig. 1. The flow domain is bounded in the y direction (a is the size of the domain in the y direction) and is infinite in the x direction. Conservative solute transport in this domain can be described by the 2D advection-dispersion equation

$$\partial c/\partial t + v \cdot \nabla c = D\nabla^2 c \tag{1}$$

subject to no-flux boundary conditions

$$\left.\frac{\partial c}{\partial y}\right|_{y=0,a} = 0 \tag{2}$$

at the top and bottom of the domain. The advection velocity is in the x direction and only depends on the coordinate y. It satisfies Darcy's law $v(y) = -K(y)\partial h/\partial x$, where $K(y)$ is random conductivity and $\partial h/\partial x$ is the constant (in time and space) head gradient. In the preceding equations, $c(x,y,t)$ is the solute concentration at position (x, y) and time t, and D is the dispersion coefficient assumed here to be constant and the same for each layer. Numerical solutions $c(x,y,t)$ via directly solving Eq. (1) can be expensive but with high fidelity.

For transport in a channel [$v(y)$ having a parabolic profile], Taylor derived an analytical expression for the dispersion coefficient [19]. Here we derive an expression for the dispersion coefficient for random velocity $v(y)$ with the prescribed mean, variance, and correlation function. For an infinite domain in the x direction or a domain with the length L, such as $L \gg a$, motivated by the original Taylor formulation [19,28], we may write the total concentration as

$$c(x,y,t) \approx c_1(x,y,t) = \bar{c}(x,t) + \eta(y)\frac{\partial \bar{c}}{\partial x}, \tag{3}$$

where $\bar{c}(x,t)$ is the cross-sectional average of total concentration $c(x,y,t)$. The cross-sectional averaging operator $\bar{\bullet}$ is defined as

$$\bar{\bullet} = \frac{1}{a}\int_0^a (\bullet)dy. \tag{4}$$

Both solutions $c_1(x,y,t)$ and $\bar{c}(x,t)$ are approximations of the high-fidelity solution $c(x,y,t)$, where $c_1(x,y,t)$ is a mid-fidelity solution with corrections on top of $\bar{c}(x,t)$ to consider the variations in y, and $\bar{c}(x,t)$ is a low-fidelity solution.

The in-plane variation function $\eta(y)$ is a measure of the velocity variation along the y direction and will be derived later. Equation (3) decomposes the total stochastic concentration solution $c(x,y,t)$ in terms of the cross-sectional average concentration $\bar{c}$ and its first-order gradient $\partial\bar{c}/\partial x$, which can be a result of homogenization [31–35]. Though a higher-order expression for the correction [in terms of the spatial derivatives of $\bar{c}(x,t)$] may be obtained [28,36] and included in Eq. (3), only the first-order correction is considered in this study. The total uncertainty in the solution $c(x,y,t)$ can be further decomposed into the ensemble contribution to the average solution $\bar{c}(x,t)$ and the configurational contribution to the variation function $\eta(y)$ [35].

Similarly, the total velocity field is decomposed into the cross-sectional average $\bar{v}$,

$$\bar{v} = \frac{1}{a}\int_0^a v(y)dy, \tag{5}$$

and velocity fluctuation v' around that average

$$v(y) = \bar{v} + v'(y), \tag{6}$$

where both $\bar{v}$ and v' are random. The velocity fluctuation v' has a zero cross-sectional average

$$\overline{v'} = \frac{1}{a}\int_0^a v'(y)dy = 0. \tag{7}$$

The zero ensemble average $\langle v'\rangle = 0$ is satisfied only if the ensemble average $\langle v(y)\rangle = \langle v\rangle$ is independent of y, which is assumed in the present study.

The key part of the proposed solution method for the stochastic partial differential equation (PDE) (1) is to formulate the equations and solutions for the cross-sectional average concentration $\bar{c}(x,t)$ and in-plane variation function $\eta(y)$. The boundary condition of $c(x,y,t)$ [Eq. (2)] immediately leads to the boundary conditions for $\eta(y)$:

$$\left.\frac{\partial \eta}{\partial y}\right|_{y=0,a} = 0. \tag{8}$$

By applying the cross-sectional operator to both sides of Eq. (3), the cross-sectional average of the function $\eta(y)$ is found as

$$\bar{\eta} = \frac{1}{a}\int_0^a \eta(y)dy = 0. \tag{9}$$

Substitution of Eq. (3) into the original stochastic PDE (1) and applying the cross-sectional average operator to both sides of Eq. (1) leads to the equation for $\bar{c}(x,t)$:

$$\frac{\partial \bar{c}}{\partial t} + \left(\bar{v} - D\overline{\frac{\partial^2 \eta}{\partial y^2}}\right)\frac{\partial \bar{c}}{\partial x} = (D - \overline{v\eta})\frac{\partial^2 \bar{c}}{\partial x^2}. \tag{10}$$

It is evident that the reduced model for $\bar{c}(x,t)$ [Eq. (10)], a one-dimensional stochastic PDE, is easier to solve than the original Eq. (1). According to Eq. (7), the statistical ensemble average of velocity fluctuation is

$$\langle v'(y)\rangle = \frac{1}{a}\int_0^a \langle v(y)\rangle dy - \langle v(y)\rangle, \tag{11}$$

where the operator $\langle\bullet\rangle$ represents the statistical ensemble average of a field variable $\bullet$.

Using the boundary condition (8), we find the conditions for $\eta(y)$,

$$\overline{\frac{\partial^2 \eta}{\partial y^2}} = \left.\frac{\partial \eta}{\partial y}\right|_{y=a} - \left.\frac{\partial \eta}{\partial y}\right|_{y=0} = 0. \tag{12}$$

By substituting Eq. (12) into Eq. (10), the equation for $\bar{c}(x,t)$ is further reduced to

$$\frac{\partial \bar{c}}{\partial t} + \bar{v}\cdot\frac{\partial \bar{c}}{\partial x} = \tilde{D}\frac{\partial^2 \bar{c}}{\partial x^2}, \tag{13}$$

where

$$\tilde{D} = D - \overline{v\eta} = D - \overline{v'\eta} \tag{14}$$

is a stochastic scalar function representing the effective dispersion coefficient for $\bar{c}(x,t)$ due to the random velocity $v(y)$. The term $\overline{v'\eta}$ represents the contribution of the nonuniform advection velocity field $v(y)$ to the dispersion.

Thus far, we have formulated the stochastic advection-dispersion equation (13) for $\bar{c}(x,t)$ with stochastic advection velocity $\bar{v}$ and stochastic effective dispersion $\tilde{D}$ that depends on the in-plane function $\eta(y)$. To derive an equation for $\eta(y)$, Eqs. (3) and (13) are substituted into the original stochastic PDE (1), which leads to

$$\frac{\partial \bar{c}}{\partial x}\left(v - \bar{v} - D\frac{\partial^2 \eta}{\partial y^2}\right) + \frac{\partial^2 \bar{c}}{\partial x^2}(v\eta - \bar{v}\eta - \overline{v\eta}) - \frac{\partial^3 \bar{c}}{\partial x^2}\eta\overline{v\eta} = 0. \tag{15}$$

Because the expansion of total concentration $c(x,y,t)$ [Eq. (3)] only retains a first-order correction, we obtain an equation for $\eta(y)$ satisfying Eq. (15) to the first order:

$$D\frac{\partial^2 \eta}{\partial y^2} = v - \bar{v} = v'. \tag{16}$$

Equation (15) needs to be satisfied to higher order if higher-order gradients are included in the original expansion of Eq. (3). By integrating Eq. (16) twice and using the boundary conditions (8) and constraint (9), we obtain the solution for $\eta(y)$:

$$\eta(y) = \frac{1}{D}\left[\int_0^y\int_0^{y_2} v'(y_1)dy_1dy_2 - \frac{1}{a}\int_0^a\int_0^y\int_0^{y_2} v'(y_1)dy_1dy_2dy\right]. \tag{17}$$

Taking the ensemble average of both sides of Eq. (17), we find that the necessary condition for

$$\langle\eta(y)\rangle = 0 \tag{18}$$

is $\langle v'\rangle = 0$.

The stochastic effective dispersion coefficient $\tilde{D}$ can be derived from Eq. (14). First, we integrate Eq. (17) by parts and the boundary condition for $\eta(y)$ in Eq. (8) to obtain

$$-\overline{v'\eta} = -D\overline{\frac{\partial^2 \eta}{\partial y^2}\eta} = D\overline{(\partial\eta/\partial y)^2}. \tag{19}$$

Substituting this into Eq. (14), we obtain the solution for $\tilde{D}$:

$$\tilde{D} = D[1 + \overline{(\partial\eta/\partial y)^2}] = D\left(1 + \frac{1}{D^2}\overline{\int_0^y v'(y_1)dy_1\int_0^y v'(y_2)dy_2}\right). \tag{20}$$

It can be seen from Eq. (20) that the stochastic effective dispersion $\tilde{D} \geqslant D$, i.e., the heterogeneity (fluctuations) in advective velocity $v(y)$, always enhances the effective dispersion.

Next we demonstrate the consistency of our formulation with the Taylor-Aris theory for the (deterministic) parabolic velocity profile for $v(y)$:

$$v(y) = \frac{3}{2}\bar{v}\left(1 - \frac{y^2}{(a/2)^2}\right). \tag{21}$$

Substitution of the expression (21) into Eq. (17) leads to the corresponding solution for $\eta(y)$:

$$\eta(y) = \frac{\bar{v}a^2}{60D}\left\{1 - \frac{15}{8}\left[1 - \left(\frac{y}{a/2}\right)^2\right]^2\right\}. \tag{22}$$

Then the effective dispersion coefficient $\tilde{D}$ can be computed via substitution of Eqs. (21) and (22) into Eq. (14) as

$$\tilde{D} = (D - \overline{v'\eta}) = D\left(1 + \frac{P_e^2}{210}\right), \tag{23}$$

where the Péclet number is defined as $P_e = a\bar{v}/D$. This result exactly recovers the Taylor dispersion coefficient [19].

III. STATISTICAL PROPERTIES OF EFFECTIVE PARAMETERS

Next we study the statistical properties of $\bar{v}$ and $\tilde{D}$ in Eq. (13). The mean and variance of $\bar{v}$ can be analytically obtained for a given covariance function of stochastic velocity $v(y)$. Here we assume that $v(y)$ is statistically homogeneous and has the constant (ensemble) mean $\langle v\rangle$ and exponential covariance function

$$\langle v(y_1)v(y_2)\rangle = \langle v(y)\rangle^2 + \sigma^2\exp\left(-\frac{|y_1 - y_2|}{\lambda}\right), \tag{24}$$

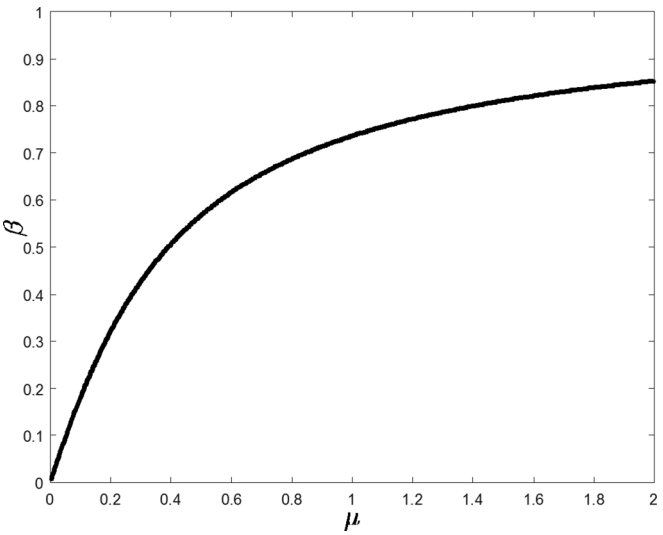

FIG. 2. Fluctuation of variance ratio β with correlation length μ. The variance $\sigma_{\bar{v}}^2 < \sigma^2$ but approaches σ^2 when $\mu \to \infty$.

where σ^2 is the variance of velocity fluctuation and λ is the correlation length. Then the ensemble mean and variance of $\bar{v}$ are given by [34]

$$\langle \bar{v} \rangle = \langle v \rangle, \quad \sigma_{\bar{v}}^2 = \langle \bar{v}^2 \rangle - \langle \bar{v} \rangle^2 = 2\sigma^2 \mu^2 (e^{-1/\mu} + 1/\mu - 1), \tag{25}$$

respectively, where $\mu = \lambda/a$ is the dimensionless correlation length. Figure 2 shows the variation of the nondimensional ratio $\beta = \sigma_{\bar{v}}^2/\sigma^2$ with the correlation length μ, where β approaches 1 with increasing correlation length μ or $\sigma_{\bar{v}}^2 \to \sigma^2$ when $\mu \to \infty$.

The statistical mean of the effective dispersion $\tilde{D}$ can be obtained from Eq. (20) as

$$\frac{\langle \tilde{D} \rangle}{D} = 1 + \frac{\gamma a^2 \sigma^2}{D^2}, \tag{26}$$

where

$$\gamma = \overline{\int_0^y \int_0^y \langle v'(y_1) v'(y_2) \rangle dy_1 dy_2} \Big/ (a\sigma)^2 \tag{27}$$

is a dimensionless number representing the effect of velocity fluctuation on mixing enhancement. The covariance function of the velocity fluctuation $v'(y_1)$ can be related to the covariance function of $v(y)$ using Eq. (6) as

$$\langle v'(y_1) v'(y_2) \rangle = \langle v(y_1) v(y_2) \rangle + \langle \bar{v}^2 \rangle - \langle \bar{v} \cdot v(y_2) \rangle - \langle \bar{v} \cdot v(y_1) \rangle. \tag{28}$$

The final expression for γ is obtained using Eq. (28) as

$$\gamma = 4\mu^4 (e^{-1/\mu} - 1) + 4\mu^3 - \tfrac{1}{3}\mu^2 (e^{-1/\mu} + 5) + \tfrac{1}{3}\mu \tag{29}$$

and is plotted in Fig. 3 as a function of μ. This figure show that γ increases from zero to its maximum value $\gamma = 0.026$, corresponding to $\mu \approx 0.25$, and then decreases to zero for large μ.

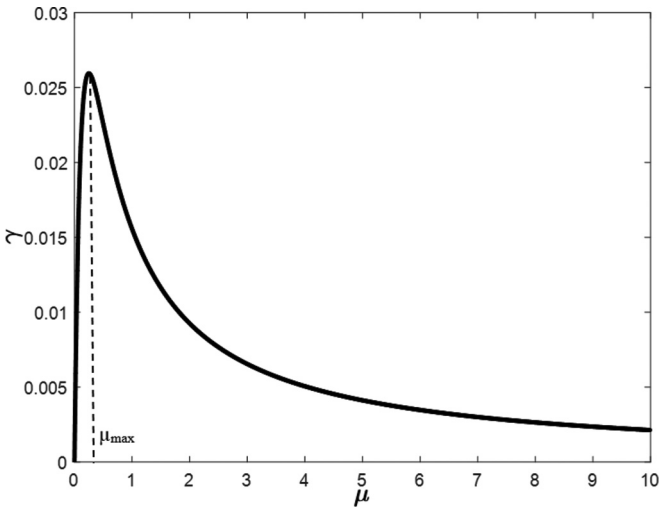

FIG. 3. Variation of enhancement in dispersion with the correlation length μ showing a stochastic spike at $\mu_{\max}$.

Let us make a comparison with the macrodispersion model by Neuman [3]. We first write the velocity as a function of permeability $k(y)$ using Darcy's law

$$v(y) = \frac{k(y)}{\upsilon\phi} g, \tag{30}$$

where $k(y)$ is the permeability field for each layer, υ is kinematic viscosity, ϕ is the porosity, and g is the force per unit mass in the x direction with a unit of acceleration. Let us assume the covariance function of $k(y)$ as

$$\langle k(y_1) k(y_2) \rangle = \langle k \rangle^2 + \sigma_k^2 \rho(|y_2 - y_1|), \tag{31}$$

where $\langle k \rangle$ and σ_k^2 are the mean and variance of the permeability and ρ is the autocorrelation function. The velocity covariance can be written as

$$\langle v(y_1) v(y_2) \rangle = \langle v \rangle^2 \left[1 + \alpha_k^2 \rho(|y_2 - y_1|) \right] \tag{32}$$

after Eq. (30), where $\alpha_k = \sigma_k / \langle k \rangle$ is the coefficient of variance for permeability field k. A comparison between Eqs. (32) and (24) leads to the relation $\sigma = \alpha_k \langle v \rangle$. The macrodispersion theory predicts the effective dispersion (in the limit of vanishing D and μ)

$$\frac{\tilde{D}_N}{D} = 1 + \frac{a\langle v \rangle}{D} \alpha_k^2 \mu, \tag{33}$$

which scales linearly with both the correlation length μ and $\langle v \rangle$. In contrast, our model (26) gives

$$\frac{\tilde{D}}{D} = 1 + \left(\frac{a\langle v \rangle}{D} \right)^2 \alpha_k^2 \gamma, \tag{34}$$

where the effective dispersion scales quadratically with $\langle v \rangle$ and is a nonlinear function of μ that exhibits a maximum at $\mu_{\max} = 0.25$, a stochastic spike referring to a sharp increase before $\mu_{\max}$ followed by a relatively slow decrease to 0 at infinity. This characteristic is also demonstrated for the stochastic heat conduction problem [34].

The correlation length $\mu_{\max}$ leading to the maximum dispersion should depend on the particular choice of covariance function ρ, but not on any other model parameters. Maximum

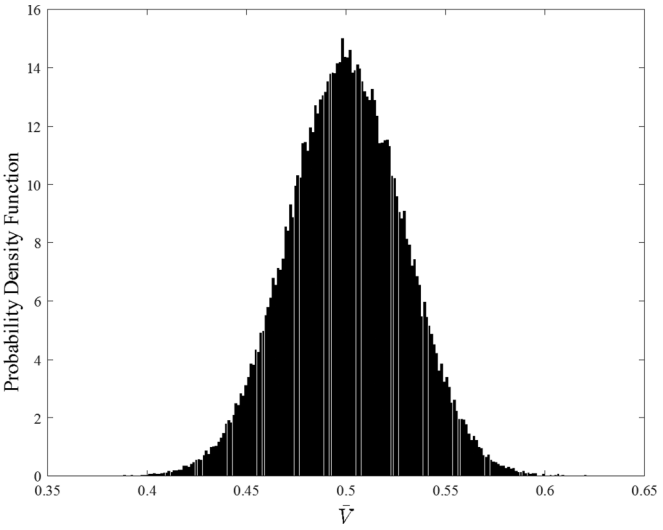

FIG. 4. Probability density function of effective velocity $\bar{v}$.

enhancement in mixing can be achieved for the stochastic velocity field $v(y)$ with a correlation length $\lambda_{\max} \approx 0.25a$, where a is the total layer thickness. This information can be useful for engineering a layered medium to achieve the maximum effect of mixing.

A quick comparison with Taylor dispersion can also be made here. Note that for the parabolic velocity profile (21), the velocity variance is

$$\sigma^2 = \overline{[v(y) - \bar{v}]^2} = \bar{v}^2/5 \tag{35}$$

and the equivalent γ from Taylor's theory is $\gamma = 1/42 \approx 0.0238$, only slightly smaller than the maximum value $\gamma = 0.026$ for the random velocity.

Finally, we perform MCSs to compute the probability distribution functions (PDFs) of $\bar{v}$, $\tilde{D}$, and $\eta(y)$. We assume that the porous medium is made of 100 layers and the velocity

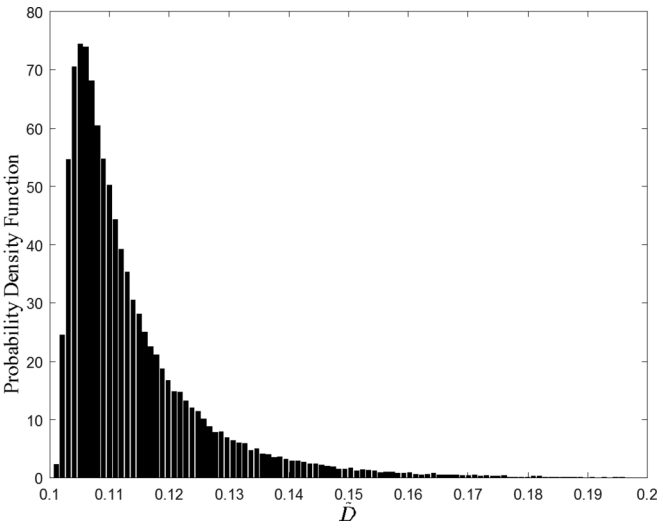

FIG. 5. Probability density function of effective dispersion $\tilde{D}$ with $D = 0.1$ corresponding to the dispersion of constant velocity. The ensemble mean $\langle \tilde{D} \rangle$ shows the enhancement in dispersion due to velocity fluctuation.

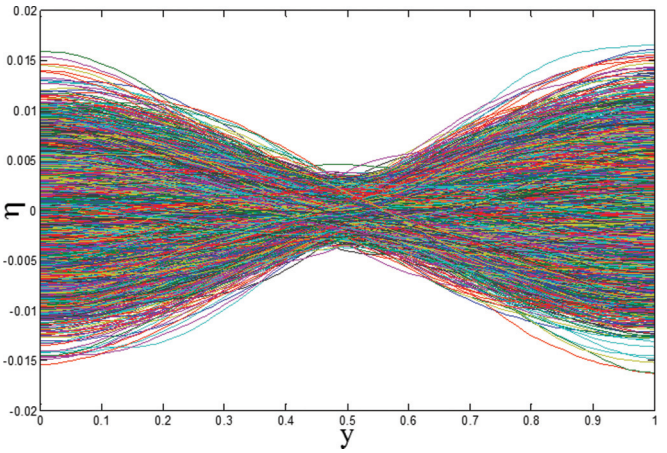

FIG. 6. Plot of in-plane variation $\eta(y)$ fluctuating with y from 10^5 samplings.

in each layer is constant with a uniform distribution defined on the interval [0,1]. Figures 4 and 5 illustrate the PDFs of $\bar{v}$ and $\tilde{D}$ with $\bar{v}$ and $\tilde{D}$ approaching Gaussian and χ^2 distributions, respectively, for small correlation length μ.

Figure 6 depicts the realizations of $\eta(y)$ obtained from the MCS. The PDFs for $\eta(y)$ at the top ($y = 1$) and middle ($y = 0.5$) of the domain are presented in Figs. 7 and 8. The PDF function for $\eta(y)$ approaches a Gaussian distribution at all locations but with a fluctuating variance that is larger at both upper and lower boundaries and smaller in the middle of the domain.

IV. NUMERICAL EXAMPLE

To investigate the accuracy of the proposed models, Eq. (1) was first fully solved by a finite-difference simulator for chosen parameters to examine flow and transport through a multilayer random media with ten layers of a total thickness $a = 1$. The diffusivity $D = 0.1$ was used and 100 realizations were generated on a 2D mesh with velocity $v(y)$ discretized into ten

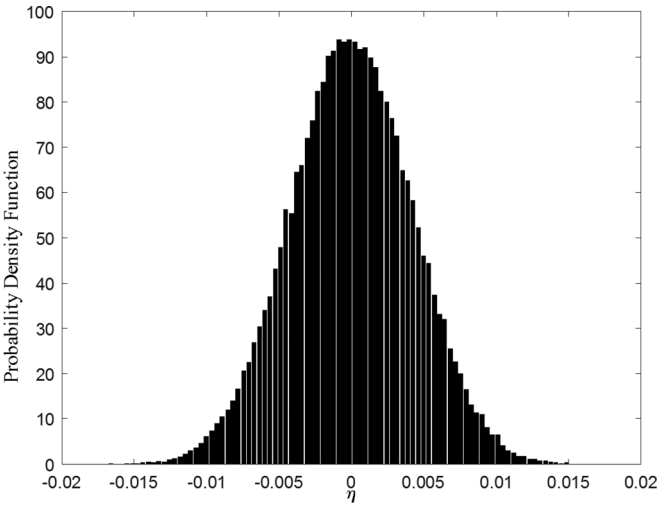

FIG. 7. Probability density distribution of $\eta(y)$ at $y = 1$.

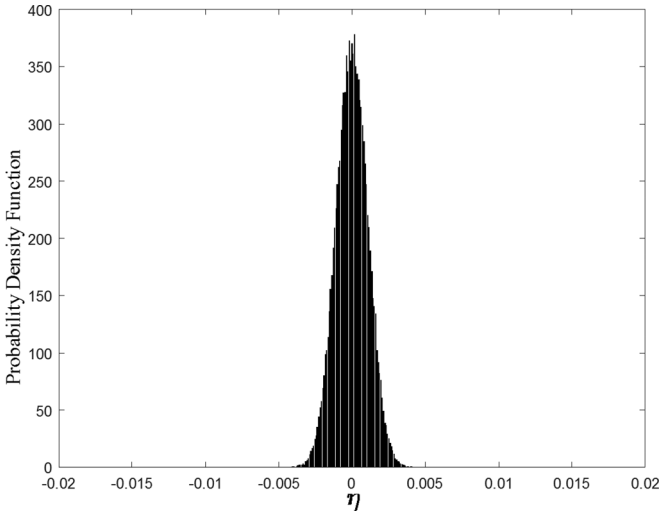

FIG. 8. Probability density distribution of $\eta(y)$ at $y = 0.5$.

random variables vertically following a Gaussian distribution with $\langle v \rangle = 1$ and a unit variance ($\sigma = 1$).

The numerical solutions obtained, i.e., the high-fidelity numerical solutions $c(x,y,t)$ by solving Eq. (1) directly, will be used as a reference for comparison. The cross-sectional average solutions $\bar{c}(x,t)$ can be obtained by solving the one-dimensional effective equation (13) with effective properties computed from Eqs. (5) and (20), respectively. The proposed model will also compute the mid-fidelity solutions $c_1(x,y,t)$ using Eq. (3) to approximate the original high-fidelity solutions $c(x,y,t)$, where the in-plane variation function η can be computed from Eq. (17) for all realizations. Variations of η in the y direction for the first two realizations $R1$ and $R2$ are plotted in Fig. 9. Finally, three solutions ($\bar{c}$, c_1, and c) with increasing fidelity are obtained for the purpose of comparison, where $\bar{c}$ is the low-fidelity and c_1 represents the mid-fidelity solutions.

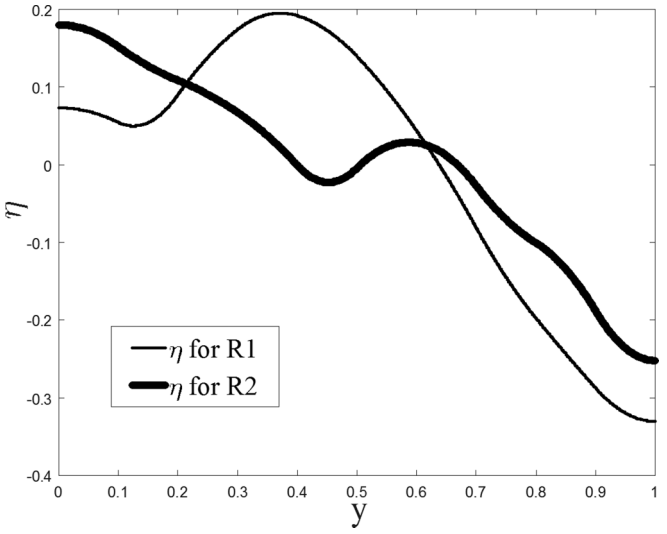

FIG. 9. Variation of η in the y direction for realizations $R1$ and $R2$.

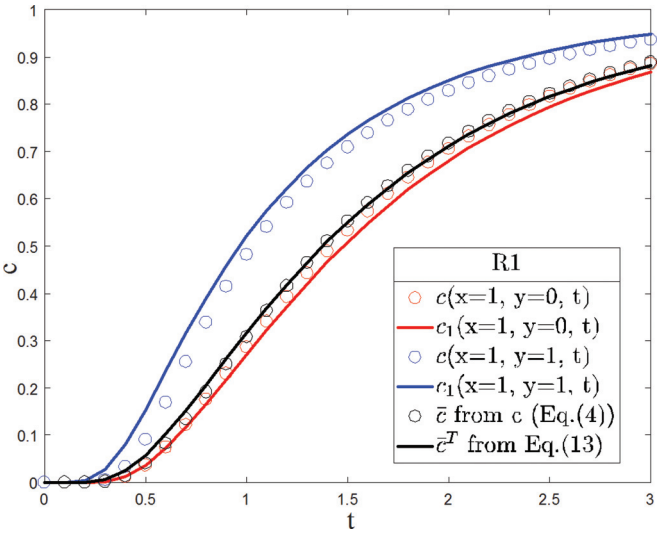

FIG. 10. Variation of concentration solutions of increasing fidelity ($\bar{c}$, c_1, and c) with time t for realization $R1$. The solution $\bar{c}^T$ is obtained by cross-sectional averaging of the high-fidelity solution c using Eq. (4).

To assess the discrepancy between $\bar{c}$, c_1, and c, a comparison of these solutions for the first two realizations is presented in Figs. 10 and 11, where the concentration variation with time t at locations ($x = 1, y = 0$) and ($x = 1, y = 1$) are plotted. For both realizations $R1$ and $R2$, solutions $\bar{c}$ solved by the effective equation (13) (black solid lines) are in very good agreement with solutions $\bar{c}^T$ obtained by a direct cross-sectional averaging of the high-fidelity solutions $c(x,y,t)$ using Eq. (4) (black circles), i.e., $\bar{c}^T(x,t) = \frac{1}{a}\int_0^a c(x,y,t)dy$. This validates our reduced model. The mid-fidelity solutions c_1 (blue and red solid lines) approximate the high-fidelity c (blue and red circles) much better than $\bar{c}$ for both realizations.

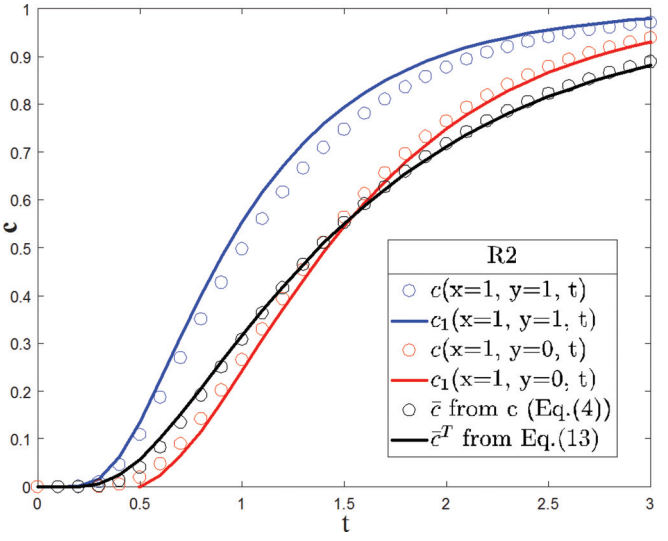

FIG. 11. Variation of concentration solutions of increasing fidelity ($\bar{c}$, c_1, and c) with time t for realization $R2$. The solution $\bar{c}^T$ is obtained by cross-sectional averaging of the high-fidelity solution c using Eq. (4).

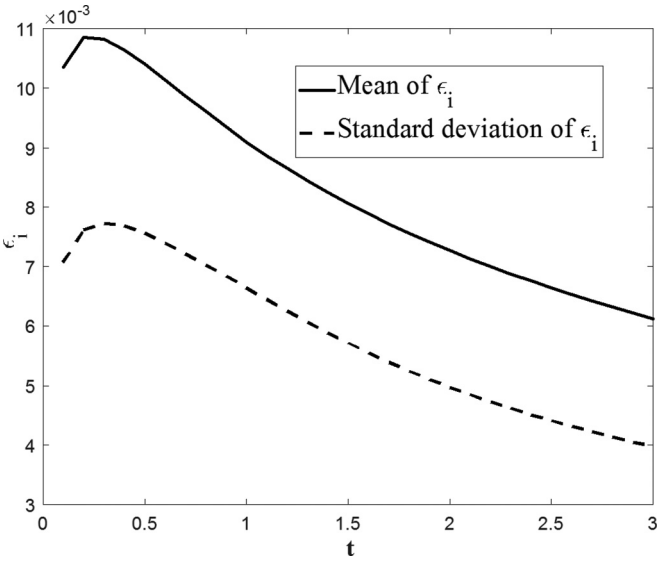

FIG. 12. Mean and standard deviation of error of $\bar{c}$ varying with time t.

In this example, the original high-fidelity solution c from the 2D stochastic model can be better approximated by the mid-fidelity model c_1 that is decomposed into a 1D low-fidelity model $\bar{c}$ and a 1D in-plane variation function η, both of which can be solved more efficiently than the original solution c. Finally, the discrepancy ε_i ($L2$ norm) between the cross-sectional average solutions $\bar{c}$ and $\bar{c}^T$ (black lines and circles in Figs. 10 and 11) can be quantified for each realization,

$$\varepsilon_i(t) = \left\| \bar{c}_i - \bar{c}_i^T \right\|_2 = \sqrt{\frac{1}{N_n} \sum_{n=1}^{N_n} \left| \bar{c}_i - \bar{c}_i^T \right|^2}, \qquad (36)$$

where i is the realization number from 1 to 100 and N_n is the total number of discretizations in the x direction. The variations of the ensemble mean and standard deviation of ε_i with time t are plotted in Fig. 12, where both the mean and deviation are decreasing with time, showing that the proposed effective model [Eq. (13)] is better at describing the long-time dynamics of solute transport with a maximum discrepancy on the order of 10^{-2}.

V. CONCLUSION

We have presented a model reduction method that results in hierarchical stochastic models for solute transport in layered porous media with random distributions of advection velocity across different layers. The model, given by Eq. (3), approximates the concentration field $c(x,y,t)$ in terms of its cross-sectional average $\bar{c}(x,t)$ and in-plane variation function $\eta(y)$ [given by Eq. (16)], where $\bar{c}(x,t)$ represents the large-scale variability of $c(x,y,t)$ and is governed by the stochastic advection-dispersion equation (13) with effective advection velocity $\bar{v}$ [given by Eq. (5)] and effective dispersion coefficient $\tilde{D}$ [given by Eq. (14) or (20)]. The small-scale variability in $c(x,y,t)$, caused by small-scale variability of the advection velocity $v(y)$, is captured by the in-plane function $\eta(y)$. The resulting multifidelity models can significantly reduce the problem dimensionality for efficiently solving the original expensive problem. The effect of correlation field length $v(y)$ on the enhancement in dispersion also has been analytically examined. In contrast to the linear scaling with correlation length and mean velocity from macrodispersion theory, our model predicts a nonlinear and a quadratic dependence of the effective dispersion on the correlation length and the mean velocity, respectively. A stochastic spike that can be identified with the maximum enhancement (maximum effective dispersion coefficient) was found for a correlation length at about $0.25a$. There is no enhancement (i.e., the effective dispersion coefficient is equal to the molecular diffusion coefficient) for both zero and infinitely large correlation lengths. This information can be very useful for engineering random layered porous media with the maximized effect of mixing.

ACKNOWLEDGMENTS

This research was supported by LDRD program "Exploring Multilevel Numerical Methods for Extreme-scale Computing" from Pacific Northwest National Laboratory. A.M.T. was partially supported by the DOE's Office of Biological and Environmental Research through the Pacific Northwest National Laboratory (PNNL) Subsurface Biogeochemical Research Scientific Focus Area project. PNNL is operated by Battelle for the DOE under Contract No. DE-AC05-76RL01830.

[1] K. D. Jarman and A. M. Tartakovsky, Geophys. Res. Lett. **35**, L15401 (2008).
[2] K. D. Jarman and A. M. Tartakovsky, Adv. Water Resour. **34**, 659 (2011).
[3] S. P. Neuman, Water Resour. Res. **29**, 633 (1993).
[4] X. Sanchez-Vila, A. Guadagnini, and D. Fernandez-Garcia, Math. Geosci. **41**, 323 (2009).
[5] G. I. Schueller, Arch. Appl. Mech. **75**, 755 (2006).
[6] W. K. Liu, T. Belytschko, and A. Mani, Int. J. Numer. Methods Eng. **23**, 1831 (1986).
[7] E. Vanmarcke and M. Grigoriu, J. Eng. Mech. **109**, 1203 (1983).
[8] H. Contreras, Comput. Struct. **12**, 341 (1980).
[9] R. Ghanem and S. Dham, Transp. Porous Media **32**, 239 (1998).
[10] G. Stefanou and M. Papadrakakis, Comput. Methods Appl. Mech. Eng. **193**, 139 (2004).
[11] M. Anders and M. Hori, Int. J. Numer. Methods Eng. **46**, 1897 (1999).
[12] R. Ghanem and P. Spanos, *Stochastic Finite Elements: A Spectral Approach* (Springer, Berlin, 1991).
[13] T. D. Hien and M. Kleiber, Comput. Methods Appl. Mech. Eng. **144**, 111 (1997).
[14] M. Kaminski and T. D. Hien, Int. Commun. Heat Mass Transfer **26**, 801 (1999).
[15] D. B. Xiu and G. E. Karniadakis, Int. J. Heat Mass Transfer **46**, 4681 (2003).
[16] V. Barthelmann, E. Novak, and K. Ritter, Adv. Comput. Math. **12**, 273 (2000).

[17] S. Smolyak, Sov. Math. Dokl. **4**, 240 (1963).
[18] R. E. Bellman, *Adaptive Control Processes: A Guided Tour* (Princeton University Press, Princeton, 1961).
[19] G. Taylor, Proc. R. Soc. London Ser. A **219**, 186 (1953).
[20] G. Taylor, Proc. R. Soc. London Ser. A **223**, 446 (1954).
[21] R. Aris, Proc. R. Soc. London Ser. A **235**, 67 (1956).
[22] J. R. Philip, Aust. J. Phys. **16**, 287 (1963).
[23] H. Brenner, Philos. Trans. R. Soc. London Ser. A **297**, 81 (1980).
[24] W. N. Gill and R. Sankaras, Proc. R. Soc. London Ser. A **316**, 341 (1970).
[25] R. Smith, J. Fluid Mech. **175**, 201 (1987).
[26] I. Frankel and H. Brenner, J. Fluid Mech. **204**, 97 (1989).
[27] H. B. Fischer, Annu. Rev. Fluid Mech. **5**, 59 (1973).
[28] Z. J. Xu, Chem. Eng. Commun. **200**, 853 (2013).
[29] Z. J. Xu, J. Heat Transfer **134**, 071705 (2012).
[30] D. L. Koch and J. F. Brady, J. Fluid Mech. **154**, 399 (1985).
[31] Z. J. Xu and P. Meakin, Appl. Math. Model. **37**, 8533 (2013).
[32] Z. J. Xu, Commun. Theor. Phys. **57**, 348 (2012).
[33] Z. J. Xu, Commun. Theor. Phys. **58**, 189 (2012).
[34] Z. J. Xu, R. Tipireddy, and G. Lin, Appl. Math. Model. **40**, 5542 (2016).
[35] Z. J. Xu, Appl. Math. Model. **38**, 3233 (2014).
[36] G. N. Mercer and A. J. Roberts, SIAM J. Appl. Math. **50**, 1547 (1990).